CHAPTER 6

AN *AB INITIO* STUDY OF THE RED CHROMOPHORE IN ULTRAMARINE

IN

Aspects of solid-state chemistry of fly ash and ultramarine pigments

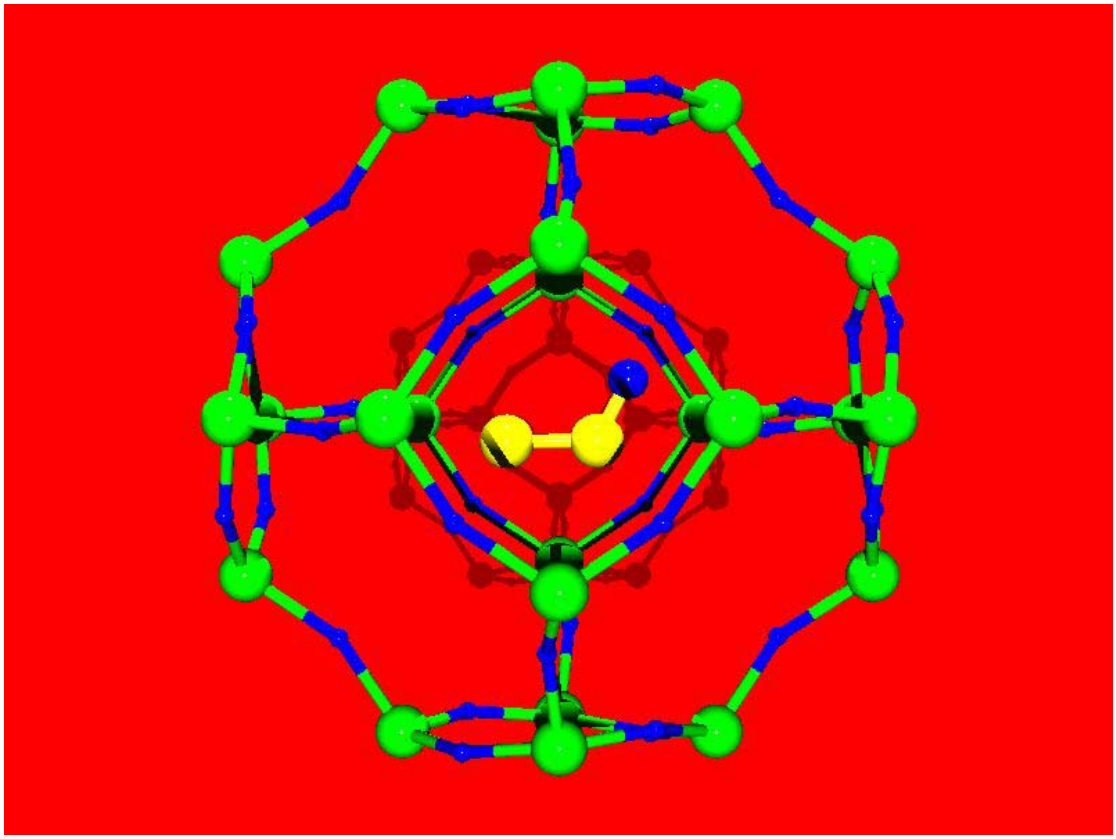

6. AN *AB INITIO* STUDY OF THE RED CHROMOPHORE IN ULTRAMARINE

6.1. Introduction

During the synthesis of ultramarine blue a green intermediate product was obtained. This green species was the result of a yellow chromophore ($S_2^{-\bullet}$) and a blue chromophore ($S_3^{-\bullet}$) present in the zeolite structure.[1-3] Wieckowksi and others[4] reported that "[u]ltramarine green can be oxidised to ultramarine blue and ultramarine red, in which sulphur is in a less negative oxidation state than in the blue ultramarine." Violet ultramarine pigments were synthesised from ultramarine blue by reaction with ammonium chloride at approximately 240 ºC in the presence of air.[1] A pink product was produced from the violet species by reaction with hydrogen chloride gas at 140 ºC.[1] Species containing chloride might, therefore be considered as possible red chromophores in ultramarine. Ultramarine red could be obtained by treating ultramarine violet at 130 - 150 ºC with nitric acid vapour. Dilute nitric acid yielded a deeper red colour.[5,6]

Based on the production of SO_2 and $S_6O_6^{2-}$ when the pigment was dissolved in acids, Hoffmann and others[7] suggested S_2O to be the chromophore in ultramarine red. Schwarz and Hofmann[8] supported this, based on an average oxidation state of between 1.25 and 1.37 for sulphur in the ultramarine red pigment. The average oxidation state was determined by the sulphur K_α X-ray fluorescence line. Tang and Brown[9] observed the Raman vibrational frequencies of S_2O in an Argon matrix at 20 K at 382, 673, and 1 157 cm^{-1}. Clark and Cobbold[2] assigned Raman bands at 352, 653.5, 674, and 1 024 cm^{-1} to the red chromophore. The 1 024 cm^{-1} band was assumed to be a combination of the 352 and 674 cm^{-1} band. Clark and Cobbold[2] concluded that the red chromophore could not be S_2O and suggested that S_4 was the red chromophore, based on the absorption band for S_4 observed by Meyer and others.[10] Seel and others[11] concluded that the red chromophore was S_4, based on the size of the cages in the sodalite framework, the number of alkali metal atoms present in the ultramarine red pigment, and the mobility of the suspect species.

To elucidate the nature of the red chromophore the species S_3 (1,2), SOS (3), SOS^-, S_2O (4), S_2O^-, S_4, S_4^-, S_3Cl, S_3Cl^-, and S_2Cl[1,2,7,8,11] were examined by molecular

modelling. This set included both open (1), C_{2v}, and closed (2), D_{3h}, S_3 (Figure 5-1), the S_4 isomers with structures of (5) *cis* chain (C_{2v}), (6) gauche chain (C_2), (7) *trans* chain (C_{2h}), (8) puckered ring (D_{2d}), (9) butterfly (D_{2d}), (10) tetrahedral (geometry optimised) (D_{2d}), (11) tetrahedral (non geometry optimised) (T_d), (12) double triangle (D_{4h}), (13) square planar (D_{4h}), (14) rectangle (D_{2h}), (15) exocyclic (C_{2v}), (16) branched chain (D_{3h}), (17) pyramidal (C_s), (18) bent exocyclic (C_s) (Figure 5-2), including the negative ions of these species, gauche (19), c*is*, (20) *trans* (21), and branched chain (22) S_3Cl isomers and their negative ions, as well as S_2Cl (23) (Figure 6-1).

6.2. Experimental data

Experimental data were required as a benchmark for comparison with the modelling studies. Electron paramagnetic resonance showed that the red chromophore was less paramagnetic than the chromophores in ultramarine blue,[7,12] but this was questioned.[13] An electronic absorption band for the ultramarine red occurred at 520 nm.[2,3,7,8,11] Vibrational modes were observed in both infrared (1 210 cm^{-1})[8] and Raman (352, 654, 674, and 1 024 cm^{-1})[2,3] spectra.

Phillips and others[14] found that S_2O had only one transition in the 230 - 600 nm region between 280 and 340 nm, and was colourless. The infrared spectrum of S_2O contained stretching frequencies at 679 and 1 165 cm^{-1} [15,16] and a bending vibration at 388 cm^{-1}.[16] Hopkins and others[17] found infrared absorptions for S_2O at 1 165, or 1 125 cm^{-1} depending on the matrix in which the spectra were obtained.

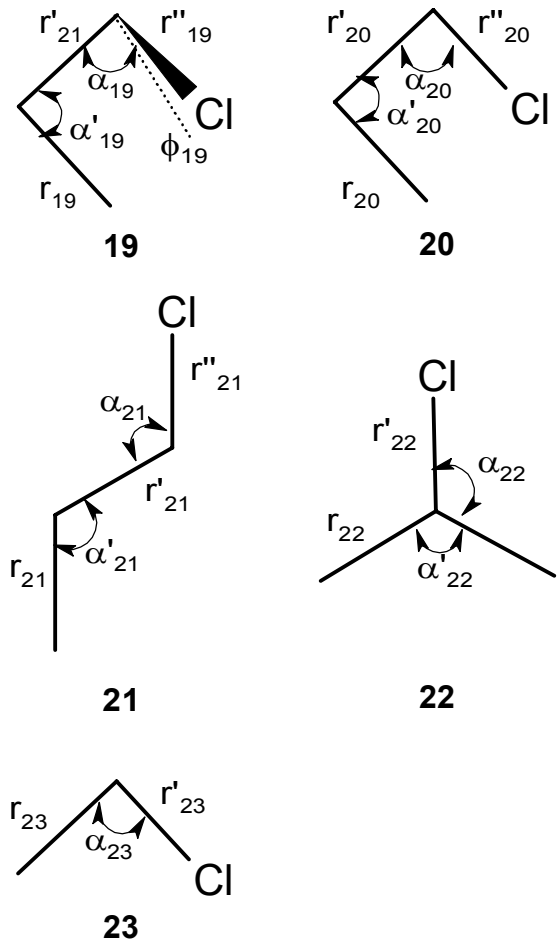

Figure 6-1: S_3Cl and S_2Cl isomers: (19) Gauche (C_1), (20) cis (C_s), (21) trans (C_s), (22) branched chain (C_s), (23) S_2Cl (C_s)

The neutral S_4 species had an absorption band at 520 nm.[18-21] S_4 had been studied in the vapour phase[18-20,22,23] and in the frozen[10,19,21] state. The results were interpreted in terms of different isomers (Figure 5-2), such as *cis* chain,[18,21] bent exocyclic,[18,22] gauche chain,[20] *trans* chain,[20-23] branched chain,[20] puckered ring,[10] or planar ring[10] (Table 6-1).

Brabson and others concluded from the infrared spectrum of S_3 in a solid argon matrix,[21] that the structure of S_3 was the C_{2v} open geometry, with an angle of 116 ± 2º. They observed an electronic absorption between 350 and 440 nm with vibrational progressions of 340 and 450 cm^{-1}, in addition to an infrared band at 680 cm^{-1} and a Raman vibrational band at 583 cm^{-1}. Other researchers also observed the vibrational progressions in the electronic spectrum[18,19] and the Raman

spectra.[9] Lenain and others[24] studied the Raman spectra of S_3 and concluded that the C_{2v} isomer was the observed species, with an absorption maximum at 395 nm and observed Raman bands at 575, 256, and 656 cm^{-1}.

Table 6-1: Experimental Characteristics of S_4

Reference	Suggested Structure	Assignment	Infrared cm^{-1}	Raman cm^{-1}	UV/Vis nm
[17]	None			668,688 601 440	
[22]	*Trans*	ν_s		678	530
		ν_c		575	
		δ_s		303	
[18,21]	*Cis* and/or *trans*, or bent exocyclic	ν_{as}	662		518
		δ_{as}			
		τ			
[22]	Bent exocyclic	$\nu_{exo\ ring}$		635	560-660
		ν_s		575	
		ν'_s		400	
[18,21]	*Cis* and/or *trans*, or bent exocyclic		642		560-660
[10]	Chain		668		530
			483		
			320		
			270		
	Puckered or planar ring		647		
[19]	None				530
[23]	*Trans*	δ_s		303	
		ν_c		575	
		ν_s		680	

6.3. Molecular Modelling

The potential energy surface was inspected for different S_4, S_4^-, S_3, S_3Cl, and S_3Cl^- isomers in an effort to find the most favourable isomer of each species.

6.4. Results

For S_3, the open (1), C_{2v}, isomer was calculated to be the most stable, after geometry optimisation (Table 6-2). The calculated vibrational frequencies of the open and closed S_3 isomers discounted both of them as possible chromophores in ultramarine

red (Table 6-3 and Table 6-4), since no infrared vibration is expected above 1 200 cm^{-1}. Furthermore, the calculated high frequency bands, 654 and 737 cm^{-1}, were too far apart from each other, to be assigned to the observed bands at 654 and 674 cm^{-1}.[2,3] Neither S_3 isomer had calculated electronic transitions in the expected region (Table 6-5).

The geometries of the S_4 isomers (Figure 5-2) were optimised (Table 6-6). Some isomers were found to be less likely to be observed than others. Diradicals were expected for the chain structures, therefore multiplicities of both 1 and 3 were evaluated for all S_4 species. The *cis* chain (5) geometry optimised to the gauche chain (6), which was surprising, in light of the relative energy results (Table 6-7). The butterfly (9) and tetrahedron structures (10,11) optimised to the puckered ring (8) geometry. The double triangle (12) was quantum mechanically equivalent to the square planar (13) structure, indicated by the total charge density plot (Figure 6-2). The exocyclic (15) structure did not yield a proper geometry, but rather seemed to dissociate into two S_2 molecules. Furthermore, the pyramidal branched chain (17) optimised to a structure with an unreasonable charge density distribution. Suitable geometric parameters were chosen for these isomers to reflect the similarity to the other structures that did optimise (Table 6-6).

Table 6-2: Bond lengths (Å) and bond angles (°)[a] for the geometry of open and closed S_3

	Singlet Open S_3 C_{2v}		**Singlet Closed S_3 D_{3h}**	**$^3B_2$ Open S_3 C_{2v}**		**$^3A_2$ Open S_3 C_{2v}**	
	r_3	**α_3**	**r_4**	**r_3**	**α_3**	**r_3**	**α_3**
This work	1.90	117	2.08			1.99	93
Average from literature[b]	1.98(2)	116.6(7)	2.12(2)	2.017	106.8	2.00(4)	93(2)
Reference	[25-33]			[29]		[26,29]	

a. The parameters are defined in Figure 5-1
b. The value given is the average from several literature values, the number in brackets denotes one standard deviation of the mean

Table 6-3: Vibrational frequencies in cm^{-1} of open S_3 (1)

Mode	Description	Symmetry	Rice[32]	Raghavachari MP2/6-31G*[29]	Raghavachari HF/3-21G*[29]	This Work	Spectro-scopic Activity[a]
ν_1	Symmetric stretch	a_1	668	577	680 (645)	654 (627)	R, IR
ν_2	Bending	a_1	287	263	300 (229)[b]	294 (211)	R, IR
ν_3	Antisymmetric stretch	b_2	769	758	783 (530)	737 (490)	R, IR

a. R: Raman active, IR: Infrared active
b. Values in brackets are for the triplet state

Table 6-4: Vibrational frequencies in cm^{-1} of closed S_3 (2)

Mode	Description	Symmetry	Rice[32]	Raghavachari HF/3-21G*[29]	This Work	Spectroscopic Activity[a]
ν_1	Symmetric deformation	a_1'	677	651	662	R
ν_2	Stretch	e'	508	504	500	R, IR

a. R: Raman active, IR: Infrared active

Table 6-5: Electronic spectrum of several suspected chromophores in ultramarine red[a]

Transition	Position nm	Oscillator Strength	Transition	Position nm	Oscillator Strength
S_3 closed			**S_4 branched**		
1	462	0.00	1	762	0.00
2	462	0.00	2	762	0.00
S_3 open			3	708	0.00
1	2862	0.00	4	592	0.00
2	1003	0.00	5	401	0.00
3	793	0.00	6	401	0.00
4	645	0.00	**S_4 *cis***		
5	731	0.00	1	-1428	0.00
			2	1165	0.00
			3	983	0.00
S_2O			4	837	0.00
1	667	0.00	5	731	0.00
2	575	0.00	6	697	0.00
3	415	0.00	7	499	0.34
4	408	0.00	**S_4 bent exocyclic**		
SOS			1	484	0.00
1	602	0.00	**S_4 puckered ring**		
2	433	0.00	1	556	0.00
3	433	0.00	2	556	0.00
S_4 *trans*			3	441	0.00
1	-1595	0.00	4	420	0.01
2	1072	0.00	5	420	0.01
3	784	0.00			

a. Not all computed transitions are reported

Table 6-6: Bond lengths (Å) and bond angles (°)[a] for S_4

Structure Number	Structure Name	Symmetry	Structural Parameter	This Work	Average from literature[b]	References
5	Singlet *cis* S_4	C_{2v}	r_5	2.04	1.95(2)	[28,29,31,33-36]
			r'_5	2.04	2.01(2)	
			α_5	110	109(2)	
6	Singlet gauche S_4	C_2	r_6	2.04	1.99(2)	[28,34,36]
			r'_6	2.02	2.11(3)	
			α_6	92	105(1)	
			ϕ_6	99	71(12)	
7	Singlet *trans* S_4	C_{2h}	r_7	1.93	1.95(2)	[26,29,33-36]
			r'_7	1.97	2.01(3)	
			α_7	110	109(1)	
8	Puckered ring S_4	D_{2d}	r_8	2.11	2.10(3)	[26,29,33-36]
			ϕ_8	30 (86)	33(8) {86.6(5)}	
11	Tetrahedral S_4	T_d	r_{11}	2.31	2.02(3)	[28,31]
13	Square planar S_4	D_{4h}	r_{13}	2.12	2.12(5)	[28]
14	Rectangular planar S_4	D_{2h}	r_{14}	2.00	1.89(2)	[26,29,33-36]
			r'_{14}	2.50	2.538(8)	
15	Exocyclic S_4	C_{2v}	r_{15}	2.08		
			r'_{15}	2.08		
16	Branched chain S_4	D_{3h}	r_{16}	1.91	1.95(3)	[28,29,31,33-36]
17	Pyramidal S_4	C_s	r_{17}	2.04	1.995(5)	[33,34]
			ϕ_{17}	97	99(1)	
18	Bent exocyclic S_4	C_s	r_{18}	2.10	2.11(2)	[33-36]
			r'_{18}	1.95	1.95(2)	
			r''_{18}	2.09	2.09(2)	
			ϕ_{18}	105	115(3)	
5	Triplet *cis* S_4	C_{2v}	r_5	2.04	2.01(5)	[34, 36]
			r'_5	2.04	2.22(4)	
			α_5	110	107.8(6)	
6	Triplet gauche S_4	C_2	r_6	2.04	2.04(5)	[29,33,34,36]
			r'_6	2.02	2.11(4)	
			α_6	92	105.7(8)	
			ϕ_6	99	88(5)	
7	Triplet *trans* S_4	C_{2h}	r_7	1.93	2.03(3)	[34,35]
			r'_7	1.97	2.16(3)	
			α_7	110	101.6(6)	

a. The parameters are defined in Figure 5-2
b. The value given is the average from several literature values, the number in brackets denotes one standard deviation of the mean

Table 6-7: Relative Energy (kJ/mol) results of modelling S_4[a]

Structure Number	Spin Multiplicity	Structure Name	
5	Singlet	*Cis*	0
6	Singlet	Gauche	176 (2i[b])
7	Singlet	*Trans*	29
8	Singlet	Puckered ring	84
11	Singlet	Tetrahedral	649 (3i)
13	Singlet	Square planar	117 (i)
14	Singlet	Rectangular	272 (i)
15	Singlet	Exocyclic	377 (3i)
16	Singlet	Branched chain	100
17	Singlet	Pyramidal	318 (i)
18	Singlet	Bent exocyclic	88
5	Triplet	*Cis*	96 (i)
6	Triplet	Gauche	134
7	Triplet	*Trans*	213 (i)

a. The energy of the most stable isomer was set equal to zero and the other energies are reported relative to this most stable state
b. i indicates that the species has an imaginary frequency

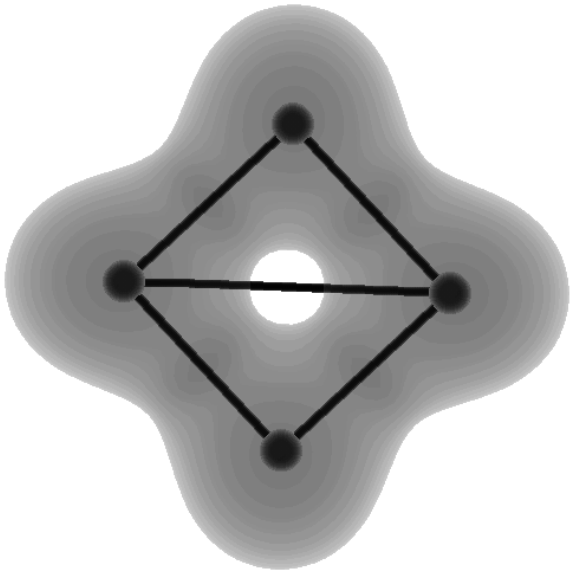

Figure 6-2: Total charge density plot of the double triangle S_4 isomer (12)

Based on the presence of negative computed infrared frequencies the tetrahedral (11), square planar (13), rectangular (14), gauche (singlet, 6), exocyclic (15), and pyramidal (17) S_4 isomers could be assigned to transition states. The gauche (6) conformer was a stable minimum in the triplet state. Only six of the proposed twelve S_4 isomers (Figure 5-2) were found to be stable minima by the *ab initio* vibrational analysis, with the 6-311G** basis set at the self-consistent field unrestricted Hartree-Fock level of theory and MP2 correlation energy. The following order of stability for the S_4 isomers was observed (Table 6-7):

cis chain (5) > *trans* chain (7) > puckered ring (8) > bent exocyclic (18) > branched chain (16) > gauche chain (triplet, 6).

Apart from the puckered ring (8) (Table 6-8) and *cis* (5) S_4 (Table 6-9) isomers, the stable S_4 isomers all had one vibrational frequency large enough to be considered as the equivalent of the observed Raman bands, but none had two of these high energy vibrations (Tables 6-8 to 6-13). None reached the observed 1 210 cm^{-1} of the infrared spectrum.[8]

A Lewis diagram of a four membered chain of sulphur atoms (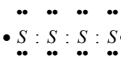) was sufficient to indicate the diradical nature of the chain.[7,8] Rings, however, were expected to have fully paired electrons.[7,19,28] Despite this *cis* (5) S_4 was the best candidate for the red chromophore, based on a calculated electronic transition at 499 nm (Table 6-5)

Table 6-8: Vibrational frequencies in cm^{-1} of puckered ring S_4 (8)

Mode	Description	Symmetry	Frequency	Spectroscopic Activity[a]
ν_1	Ring stretch	a_1	563	R
ν_2	Pucker	a_1	192	R
ν_3	Ring deformation	b_1	532	R
ν_4	Ring deformation	b_2	361	R, IR
ν_5	Ring deformation	e	509	R, IR

a. R: Raman active, IR: Infrared active

Table 6-9: Vibrational frequencies in cm^{-1} of singlet cis S_4 (5)

Mode	Description	Symmetry	Frequency	Spectroscopic Activity[a]
ν_1	Central stretch	a_1	502	R, IR
ν_2	Symmetric stretch	a_1	459	R, IR
ν_3	Symmetric deformation	a_1	151	R, IR
ν_4	Torsion	a_2	244	R
ν_5	Antisymmetric stretch	b_2	391	R, IR
ν_6	Antisymmetric deformation	b_2	322	R, IR

a. R: Raman active, IR: Infrared active

Table 6-10: Vibrational frequencies in cm^{-1} of singlet branched chain S_4 (16)

Mode	Description	Symmetry	Frequency	Spectroscopic Activity[a]
ν_1	Symmetric stretch	a_1'	500	R
ν_2	Out-of-plane	a_2''	282	IR
ν_3	Antisymmetric stretch	e'	700	R, IR
ν_4	Symmetric deformation	e'	272	R, IR

a. R: Raman active, IR: Infrared active

Table 6-11: Vibrational frequencies in cm^{-1} of trans *S_4 (7)*

Mode	Description	Symmetry	Frequency	Spectroscopic Activity[a]
ν_1	Symmetric stretch	a_g	661	R
ν_2	Central stretch	a_g	596	R
ν_3	Symmetric deformation	a_g	269	R
ν_4	Torsion	a_u	90	IR
ν_5	Antisymmetric stretch	b_u	557	IR
ν_6	Antisymmetric deformation	b_u	160	IR

a. R: Raman active, IR: Infrared active

Table 6-12: Vibrational frequencies in cm^{-1} of bent exocyclic S_4 (18)

Mode	Description	Symmetry	Frequency	Spectroscopic Activity[a]
ν_1	Basal stretch	a'	622	R, IR
ν_2	Exocyclic stretch	a'	563	R, IR
ν_3	Symmetric stretch	a'	463	R, IR
ν_4	Wagging	a'	245	R, IR
ν_5	Antisymmetric stretch	a''	427	R, IR
ν_6	Twist	a''	200	R, IR

a. R: Raman active, IR: Infrared active

Table 6-13: Vibrational frequencies in cm^{-1} of triplet gauche S_4 (6)

Mode	Description	Symmetry	Frequency	Spectroscopic Activity[a]
ν_1	Central stretch	a	605	R, IR
ν_2	Symmetric stretch	a	508	R, IR
ν_3	Symmetric bend	a	269	R, IR
ν_4	Torsion	a	64	R, IR
ν_5	Antisymmetric stretch	b	520	R, IR
ν_6	Antisymmetric bend	b	288	R, IR

a. R: Raman active, IR: Infrared active

Apart from the gauche S_4 (6) triplet state, none of the other triplet state S_4 isomers turned out to be stable minima (Table 6-14). The geometries were not re-optimised for the S_4^- isomers. The S_4 geometries were used (Table 6-15), and these compare well with other data.[33] None of the S_4^- isomers (Table 6-16) were characterised as stable minima. This observation implied that S_4^- was not supported by *ab initio* computation to be a suitable chromophore in ultramarine red.

After geometry optimisation (Table 6-17), the gauche chain was found to be the most stable isomer for S_3Cl (19, Table 6-18). The branched (22) chain had a substantially higher energy, but was a stable♦ minimum (Table 6-18). For S_3Cl^-, only the branched chain was a stable minimum (Table 6-18). S_2Cl (23) turned out to be a stable minimum as well. None of the species containing chlorine had computed vibrational frequencies (Tables 6-19 to 6-21) in the region of the observed[2,3] 654 cm^{-1}, or the 674 cm^{-1} bands in the Raman spectra of ultramarine red. These species were therefore not suitable candidates as the chromophore in ultramarine red.

♦ A stable minimum denotes a local or global minimum on the energy surface being inspected and does not include transition states, which are characterised by imaginary minima.

Table 6-14: Relative energy results of modelling the triplet state of S_4[a]

Structure Number	Structure Name	Relative Energy kJ/mol
6	Triplet puckered ring S_4	121 (2i[b])
9	Triplet tetrahedral S_4	485 (3i)
13	Triplet square planar S_4	13 (2i)
14	Triplet rectangular planar S_4	0 (4i)
15	Triplet exocyclic S_4	326 (2i)
16	Triplet branched chain S_4	146 (3i)
17	Triplet pyramidal S_4	142 (i)
18	Triplet bent exocyclic S_4	167 (2i)

a. The energy of the most stable isomer was set equal to zero and the other energies are reported relative to this most stable state
b. i indicates that the species has an imaginary frequency

Table 6-15: Bond lengths (Å) and bond angles (°)[a] of S_4^-

Structure Number	Structure Name	Symmetry	Structural Parameter	Zakrzewski HF/6-31+G*[33]	This Work
5	*Cis* S_4^-	C_{2v}	r_5	1.952	2.04
			r'_5	2.056	2.04
			α_5	114.28	110
7	*Trans* S_4^-	C_{2h}	r_7	2.016	1.93
			r'_7	2.022	1.97
			α_7	107.51	110
14	Rectangular planar S_4^-	D_{2h}	r_{14}	1.927	2.00
			r'_{14}	2.665	2.50
16	Branched chain S_4^-	D_{3h}	r_{16}	1.990	1.91
17	Pyramidal S_4^-	C_s	r_{17}	2.176	2.04
			ϕ_{17}	110.93	97
18	Bent exocyclic S_4^-	C_s	r_{18}	2.054	2.10
			r'_{18}	2.022	1.95
			r''_{18}	2.794	2.09
			ϕ_{18}	112.87	105

a. The parameters are defined in Figure 5-2

Table 6-16: Relative Energy results of modelling S_4^-

Structure Number	Structure Name	Relative Energy kJ/mol[a]	Zakrzewski HF/6-31+G*[b 33]
5	*Cis* S_4^-	243 (2i)	
6	Gauche S_4^-	84 (i)	ND
7	*Trans* S_4^-	0 (2i)	
8	Puckered square S_4^-	167 (2i)	ND
11	Tetrahedral S_4^-	715 (4i)	ND
13	Square planar S_4^-	163 (3i)	ND
14	Rectangular planar S_4^-	92 (3i)	i
15	Exocyclic S_4^-	393 (4i)	ND
16	Branched chain S_4^-	79 (i)	i
17	Pyramidal S_4^-	96 (2i)	i
18	Bent Exocyclic S_4^-	188 (3i)	i

a. i indicates that the structure has at least one imaginary frequency
b. The relative energies are not provided in the cited reference, but the result of the vibrational analysis is included

Table 6-17: Bond lengths (Å) and bond angles (°) of SOS, S_2O, S_3Cl, and S_2Cl

Structure Number	Structure Name	Symmetry	Structural Parameter[a]	This Work
3	SOS	C_{2v}	r_3	1.68
			α_3	74
4	S_2O	C_s	r'_4	1.87
			r_4	1.43
			α_4	117
19	Gauche S_3Cl	C_1	r_{19}	2.00
			r'_{19}	2.05
			r''_{19}	2.04
			α_{19}	104
			α'_{19}	108
			ϕ_{19}	84
20	*Cis* S_3Cl	C_s	r_{20}	2.00
			r'_{20}	2.05
			r''_{20}	2.04
			α_{20}	104
			α'_{20}	108
21	*Trans* S_3Cl	C_s	r_{21}	2.00
			r'_{21}	2.05
			r''_{21}	2.04
			α_{21}	104
			α'_{21}	108
22	Branched S_3Cl	C_s	r_{22}	2.04
			r'_{22}	2.01
			α_{22}	92
			α'_{22}	92
23	S_2Cl	C_s	r_{23}	1.95
			r'_{23}	2.05
			α_{23}	108

a. The parameters are defined in Figures 5-1 and 6-1

Table 6-18: Relative energy results of modelling S_2O, SOS, S_3Cl, and S_3Cl^-

Structure Number	Structure Name	Relative Energy kJ/mol[a]
3	SOS singlet	256
4	S_2O singlet	69
3	SOS triplet	526 (i[b])
4	S_2O triplet	313
3	SOS^-	313 (i)
4	S_2O^-	0
19	Gauche S_3Cl	0
20	*Cis* S_3Cl	180 (3i)
21	*Trans* S_3Cl	29 (i)
22	Branched S_3Cl	163
19	Singlet gauche S_3Cl^-	-151 (i)
20	Singlet *cis* S_3Cl^-	-79 (i)
21	Singlet *trans* S_3Cl^-	-100 (i)
22	Singlet branched S_3Cl^-	0
19	Triplet gauche S_3Cl^-	59 (2i)
20	Triplet *cis* S_3Cl^-	29 (2i)
21	Triplet *trans* S_3Cl^-	33 (3i)
22	Triplet branched S_3Cl^-	184 (2i)

a. The energy of the most stable isomer was set equal to zero for each subgroup and the other energies are reported relative to this most stable state for that subgroup
b. i indicates that the species has an imaginary frequency

Table 6-19: Vibrational frequencies in cm^{-1} of branched S_3Cl (22)

Mode	Description	Symmetry	Doublet S_3Cl	Singlet S_3Cl^-	Spectroscopic Activity[a]
ν_1	S-S(-S) symmetric stretch	a''	524	479	R, IR
ν_2	S-Cl stretch	a'	562	556	R, IR
ν_3	S-S-S bending	a'	37	259	R, IR
ν_4	Symmetric deformation	a'	293	292	R, IR
ν_5	Antisymmetric deformation	a''	409	459	R, IR
ν_6	S-S-Cl bending	a''	238	237	R, IR

a. R: Raman active, IR: Infrared active

Table 6-20: Vibrational frequencies in cm^{-1} of singlet gauche S_3Cl^- (19)

Mode	Description	Symmetry	Frequency	Spectroscopic Activity[a]
ν_1	S-S and S-Cl antisymmetric stretch	a	558	R, IR
ν_2	S-S and S-Cl symmetric stretch	a	549	R, IR
ν_3	Central stretch	a	518	R, IR
ν_4	Antisymmetric bend	a	257	R, IR
ν_5	Symmetric bend	a	196	R, IR
ν_6	Torsion	a	64	R, IR

a. R: Raman active, IR: Infrared active

Table 6-21: Vibrational frequencies in cm^{-1} of S_2Cl (23)

Mode	Description	Symmetry	Frequency	Spectroscopic Activity[a]
ν_1	S-S stretch	a'	578	R, IR
ν_2	S-Cl stretch	a'	530	R, IR
ν_3	Bending	a'	241	R, IR

a. R: Raman active, IR: Infrared active

The experimental geometry for S_2O was determined from the microwave spectrum to be r(S-O) = 1.46 Å, r(S-S) = 1.88 Å and the S-S-O angle to be 118°,[37] which compared well with the currently determined geometry (1.43 Å, 1.87 Å, 117°) (Table 6-17). S_2O^- was determined to be the most stable S_2O structure (Table 6-18) with vibrational frequencies larger than expected (Table 6-22). The calculated vibrational bands for S_2O (Table 6-22) were scaled by a factor of 0.87 as suggested by Brabson and others.[21] This procedure yielded vibrational transitions at 382, 666, and 1 180 cm^{-1}, in close agreement with three of the four observed bands for the ultramarine red chromophore. S_2O was, however, predicted to be colourless (Table 6-5), and was observed to be colourless.[11,14] The SOS possibility was also negated by its vibrational frequencies (Table 6-23).

Table 6-22: Vibrational frequencies in cm^{-1} of S_2O (4)

Mode	Description	Symmetry	Doublet S_2O^-	Singlet S_2O	Triplet S_2O	Spectroscopic Activity[a]
ν_1	S-O stretch	a'	1401	1357	1342	R, IR
ν_2	S-S stretch	a'	796	766	742	R, IR
ν_3	Bending	a'	344	440	154	R, IR

a. R: Raman active, IR: Infrared active

Table 6-23: Vibrational frequencies in cm^{-1} of singlet SOS (3)

Mode	Description	Symmetry	Frequency	Spectroscopic Activity[a]
ν_3	Bending	a_1	592	R, IR
ν_2	Antisymmetric stretch	b_2	657	R, IR
ν_1	Symmetric stretch	a_1	907	R, IR

a. R: Raman active, IR: Infrared active

6.4.1. Modelling the Cavities in the Ultramarine Structure

The volumes of the cavities of the β-cage of ultramarine blue,[38] and several sodalite structures, which also contain β-cages,[39-43] were calculated using the method and atomic-ionic radii of Gavezzotti,[44] Bondi[45] and Shannon.[46] The details of the computer algorithm can be found in Appendix A2. The volumes of the sulphur species considered (Table 6-24) were smaller than the volumes of the cavities in the sodalite structure (Table 6-25). The volumes of the cavities were calculated taking the counter ions into account, and represent the maximum volume available to the chromophore. The small percentage difference for the volumes calculated by the HyperChem Quantitative Structure-Activity Relationships (QSAR) and the current method indicated the reliability of the current method (Tables 6-24 and 6-25). The volume of the crystal cavity was approximated as a truncated octahedron in the crystal structure, by Equation 6-1:

$$V = \frac{2}{9}\left[4a^2b + 3a^2c - 2b^3\right] \qquad \textbf{(6-1)}$$

with

V: volume of the truncated octahedron as an approximation of the available volume in sodalite structures, assuming that the octahedron was formed by two regular square pyramids and that the truncation was done by subtracting a smaller regular square pyramid from the octahedron.

a: distance between two tetrahedral atoms on opposite sides of the six-membered tetrahedral ring, the size of the base of the original octahedron.

b: distance between two tetrahedral atoms on opposite sides of the four-membered tetrahedral ring, the size of the base of the subtracted octahedron.

c: distance between the base plane of the original octahedron and the base plane of the subtracted octahedron.

Table 6-24: Volume (Å^3) of the modelled species

Structure Number	Molecule	QSAR[a]	This Work	Difference % QSAR
1	Open S_3	61.300	61.00	0.5
2	Closed S_3	59.485	59.21	0.5
3	SOS	47.633	47.42	0.4
4	S_2O	47.299	47.07	0.5
5	*Cis* S_4	80.363	79.99	0.5
6	Gauche S_4	79.717	80.12	-0.5
7	*Trans* S_4	78.433	78.10	0.4
9	Puckered ring S_4	78.433	76.47	2.5
10	Tetrahedral S_4	77.733	77.54	0.3
13	Square S_4	77.122	76.74	0.5
14	Rectangular S_4	79.751	79.39	0.5
15	Exocyclic S_4	78.034	77.68	0.4
16	Branched S_4	77.556	77.19	0.5
17	Pyramidal S_4	80.302	79.98	0.4
18	Bent exocyclic S_4	77.229	76.99	0.3
19	Gauche S_3Cl	79.271	78.99	0.4
20	*Cis* S_3Cl	78.886	78.50	0.5
21	*Trans* S_3Cl	79.263	78.90	0.5
22	Branched S_3Cl	78.416	78.08	0.4
23	S_2Cl	60.293	60.04	0.4

a. QSAR: Quantitative Structure-Activity Relationships in HyperChem[47]

6.5. Discussion

The optimised geometries for the different isomers of S_3 (1,2) fell within the range of previously determined geometrical parameters (Table 6-2).[25-33] The calculated vibrational frequencies were similar to those of previous studies.[29,32] The question of whether the open, C_{2v},[25,26,29,30,32,33] or closed, D_{3h},[32,33,35,48,49] S_3 isomer was the more stable seemed to be an open one, since, depending on the methodology applied to the problem, several methods gave contradictory results. The open (1), C_{2v}, S_3 isomer was calculated to be the most stable isomer in this work. The fact that the closed (2), D_{3h}, S_3 isomer had an energy only 42 kJ/mol higher than the open isomer, suggested that both these isomers should be observable at approximately 723 K.[50,51]

Table 6-25: Approximations of the volumes (Å^3) of the cavities in sodalite structures

	Ref	This Work			QSAR	Difference (%)	Crystal Structure[a]
		Total volume	Volume occupied by the atoms	Cavity volume			
AM1 Cage Si[b]		1014.21	840.83	184.00	844.92	0.5	231.1
AM1 Cage Al[c]		1324.59	1196.76	139.12	1202.56	0.5	231.1
Modified Tarling[d]	[38]	1323.17	1208.37	126.07	1215.15	0.6	215.8
Nielsen	[39]	1195.83	1060.83	146.20	1066.07	0.5	227.4
Nielsen	[39]	1181.91	1053.60	139.44	1059.15	0.5	221.6
Nielsen	[39]	1172.18	1048.84	134.40	1054.21	0.5	217.5
Felsche	[42]	1169.25	1045.47	135.27	1050.48	0.5	213.1
Löns	[43]	1168.57	1047.87	131.82	1053.15	0.5	217.0
Werner	[41]	1117.95	1017.64	110.60	1022.89	0.5	198.9
Werner	[41]	1136.75	1028.52	118.79	1033.36	0.5	205.2
Werner	[41]	1150.24	1036.56	124.43	1041.56	0.5	209.8
Werner	[41]	1171.47	1048.66	133.86	1054.32	0.5	217.1
Mead	[40]	1195.68	1059.83	147.24	1066.04	0.6	226.5
Mead	[40]	1199.59	1061.47	149.53	1066.79	0.5	228.4
Mead	[40]	1196.62	1060.02	148.05	1065.80	0.5	226.6
Mead	[40]	1203.93	1063.55	151.85	1068.64	0.5	230.0

a. The volume of the cavity in the crystal structure was approximated as a truncated octahedron, Equation 6-1.
b. The AM1 semi-empirical method of HyperChem was used to model the cage structure, where all the tetrahedral atoms were silicon atoms.
c. The same structure as b, but the silicon atoms were replaced by aluminium atoms.
d. The structure of Tarling and others,[38] was modified so that all the tetrahedral atoms were the larger aluminium atoms.

The bond angles of the gauche S_4 chain (6) were determined to be smaller than the angles presented in the literature, whereas the dihedral angle was determined to be larger[28,34,36] (Table 6-6). The angle made by the external sulphur-sulphur bond with the ring for the bent exocyclic (18) isomer was determined to be smaller than in the literature,[29,33-35] but comparable with the value determined by Kao[36] (Table 6-6). The other geometries of the other isomers compared well with those determined in the literature[26,28,29,33-36] (Table 6-6). The correspondence between the geometries (Table 6-6) was also reflected in the agreement of the vibrational frequencies (Tables 6-9 to 6-12).[21,34] Again the gauche chain parameters deviated most from the literature values.[29,34] The exocyclic stretching frequency of the bent exocyclic isomer was affected by the different geometries (Table 6-13).[22,34] The slightly longer bond distances in the currently calculated geometry of the *cis* (5) chain was reflected in a large difference in the calculated stretching frequencies(Table 6-9). [29,34]

Several S_4 isomers had in the past been calculated to be the most stable isomer, they were *cis* (5) chain,[29,31,33,34,52] puckered ring (8),[35,52] branched chain (16),[28] gauche chain (Triplet, 6),[36] and rectangular (14) (Table 6-7).[26,29] The disparity in relative energy results for S_4 (Table 6-7) could be related to the slightly different geometries considered (Table 6-6). The rectangular (14) S_4 isomer could not be considered as a stable minimum, because the current analysis showed it to be a transition state. Other researchers confirmed this conclusion. [29,33,34]

According to the computed energy of the *cis* (5) and *trans* (7) chain S_4 species (Table 6-7), both species were expected to be present in the vapour phase, since the energy difference between these species was only 29 kJ/mol, compared to the 42 kJ/mol estimated for species that contribute to the occurrence of S_4 species at 673 to 1 173 K.[50,51] The simultaneous occurrence was supported by experimental conjecture.[18,21]

The application of only a single determinant unduly favours triplet states.[36] Unfortunately no configuration interaction was allowed for the triplet state in the current investigation. This limitation did not seem to be a problem in the current computations, since most of the triplet states were transition states. The gauche chain triplet was a stable minimum, but was not considered as the most stable structure. A higher level of theory might refute this conclusion.

The lack of a stable tetrahedral state (11) was predicted by the concerted reaction approach of Landman and De Waal (Appendix F).[53] Only the *trans* (7), *cis* (5), branched (16), gauche chain (6), puckered ring (8) and bent exocyclic (18) isomers for S_4, stood the test of the vibrational analysis. The last three corresponded to structures that withstood the Woodward-Hoffmann analysis, although with the 6-311G** basis set the bent exocyclic structure was ruled out (Chapter 5). The *trans* (7) and *cis* (5) chains were conformers of the Woodward-Hoffmann allowed gauche chain (6), whereas the branched chain (16) was the more stable conformer of the Woodward-Hoffmann allowed pyramidal structure (17).

Wong and Steudel[54] used several quantum mechanical methods and concluded that *cis* (5) S_4 had a visible absorption at 527/525 nm in close agreement with the observed value of 520-530 nm[18-21] (Table 6-1), and the current calculated value of 490 nm (Table 6-5).

6.6. Conclusion

The relative volumes of the suspected chromophore species and the cavities available in the β-cages of the aluminosilicate framework, taking the counter ions into account, did not exclude any of the species from being a possible chromophore.

On vibrational spectroscopic grounds the S_4 isomers did not correspond too well with the chromophore in ultramarine red. Due to the diradical nature of sulphur chains,[8,7] the linear chain isomers of S_4 were not regarded as acceptable chromophores, since the chromophore was known to be diamagnetic.[7,12] However, the *cis* (5) S_4 chain (C_{2v}) had a calculated electronic transition at 499 nm (Table 6-5), which made it the only possible red chromophore, based on electronic transition, which was the primary consideration.

In *ab initio* computations the S_4^- isomers did not represent stable minima (Table 6-16) and were therefore not predicted to be suitable chromophores in ultramarine red.

None of the chlorine containing species (19-23) had computed vibrational frequencies (Tables 6-19 to 6-21) in the region of the observed[2,3] Raman bands of ultramarine red, and were not regarded as viable options for the ultramarine red chromophore. The current vibrational analysis of the open (1) and closed (2) S_3 isomers and SOS (3) and S_2O (4) discounted them as possible chromophores in ultramarine red (Tables 6-3, 6-4, 6-22 and 6-23).

The scaled calculated vibrational frequencies for S_2O (4) were 382, 666, and 1 180 cm^{-1}. These values were in close agreement with the observed bands for the ultramarine red chromophore. On these grounds S_2O was a likely chromophore in ultramarine red as suggested before.[8] However, S_2O is a colourless gas.[14] Since the

aluminosilicate framework was more likely to influence vibrational, rather than electronic spectra, the *cis* S_4 species, with a computed electronic transition at 499 nm, was still the best candidate as red chromophore.

REFERENCES

1 W.B. Cork, *Ultramarine pigments*, in: Industrial Inorganic Pigments, G Buxbaum (ed), 1993, p. 124-132.
2 R.J.H. Clark, D.G. Cobbold, *Inorg. Chem,* 1978, **17**(11), 3169-3174.
3 R.J.H. Clark, T.J. Dines, M. Kurmoo, *Inorg. Chem.*,1983, **22**, 2766-2772.
4 A.B. Wieckowksi, W. Wojtowitz, J. Sliwa-Niesciór, *Magn. Reson. Chem.*, 1999, **37**, 150-153.
5 J. Zeltner, *Verfahren zur Herstellung einer rothen Ultramarinfarbe*, final patent no. 1, German, 29 November 1877.
6 R. Faust, G. Knaus, U. Siemelung, *World Records in Chemistry*, translated by W.E. Russey, First, Wiley-VCH, Weinheim, 1991, p. 182.
7 U. Hofmann, E. Herzenstiel, E. Schonemann, K-H. Schwarz, *Z. anorg. allg. chem.*, 1969, **367**, 119-129.
8 K-H. Schwarz, U. Hofmann, *Z. anorg. allg. Chem.*, 1970, **378**, 152-159.
9 S-Y. Tang, C.W. Brown, *Inorg. Chem.*, 1975, **14**(11), 2856-2858.
10 B. Meyer, T. Stroyer-Hansen, *J. Phys. Chem.*, 1972, **76**(26), 3968-3969.
11 F. Seel, H-J. Güttler, A.B. Wiecowski, B. Wolf, *Z. Naturforsch.*, 1979, **34b**, 1671-1677.
12 J. Klinowski, S.W. Carr, S.E. Tarling, P. Barnes, *Nature*, 1987, **330**, 56-58.
13 N. Gobeltz-Hautecoeur, A. Domortier, B. Lede, J.P. Lelieur, C. Duhayon, Inorg. Chem., 2002, 41(11), 2848-2854.
14 L.F. Phillips, J.J. Smith, B. Meyer, *J. Mol. Spectrosc.*, 1969, **29**, 230-234.
15 A.V. Jones, *J. Chem. Phys.*, 1950, **18**(9), 1263-1268.
16 U. Blukis, R.J. Myers, *J. Phys. Chem.*, 1965, **69**(4), 1154-1156.
17 A.G. Hopkins, S-.Y. Tang, C.W. Brown, *J. Am. Chem. Soc.*, 1973, **95**(11), 3486-3494.
18 P. Hassanzadeh, L. Andrews, *J. Phys. Chem.*, 1992, **96**(16), 6579-6585.
19 B. Meyer, T. Stroyer-Hansen, T.V. Oommen, *J. Mol. Spectrsosc.*, 1972, **42**, 335-343.
20 B. Meyer, M. Gouterman, D. Jensen, T.V. Oommen, K. Spitzer, T. Stroyer-Hansen, *The Spectrum of Sulfur and its Allotropes*, In: Sulfur Trands, Advances in Chemistry series, vol. 110, American Chemical Society, Washington, 1971, p. 53-71.
21 G.D. Brabson, Z. Mielke, L. Andrews, *J. Phys. Chem.*, 1991, **95**(1), 79-86.
22 M.S. Boumedien, J. Corset, E. Picquenard, *J. Raman Spectrosc.*, 1999, **30**, 463-472.
23 E. Picquenard, M.S. Boumedien, J. Corset, *J. Mol. Struct.*, 1993, **293**, 63-66.
24 P. Lenain, E. Picquenard, J.L. Lesne, J. Corset, *J. Mol. Struct.*, 1986, **142**, 355-358.
25 W. Koch, J. Natterer, C. Heinemann, *J.Chem.Phys.*, 1995, **102**(15), 6159-6167.
26 D. Hohl, R.O. Jones, R. Car, M. Parrinello, *J. Chem. Phys.*, 1988, **89**(11), 6823-6835.
27 W.G. Laidlaw, M. Trsic, *Chem. Phys.*, 1979, **36**, 323-325.
28 B. Meyer, K. Spitzer, *J. Phys. Chem.*, 1972, **76**(16), 2274-2279.
29 K. Raghavachari, C.M. Rohlfing, J.S. Binkley, *J. Chem. Phys.*, 1990, **93**(8), 5862-5873.
30 M. Morin, A.E. Foti, D.R. Salahub, *Can. J. Chem.*, 1985, **63**, 1982-1987.
31 D.R. Salahub, A.E. Foti, V.H. Smith, Jr, *J. Am. Chem. Soc.*, 1978, **100**(25), 7847-7858.
32 J.E. Rice, R.D. Amos, N.C. Handy, T.J. Lee, H.F. Schaefer III, *J. Chem. Phys.*, 1986, **85**(2), 963-968.
33 V.G. Zakrzewski, W. von Niessen, *Theor. Chim. Acta*, 1994, **88**, 75-96.
34 G.E. Quelch, H.F. Schaefer III, C.J. Marsden, *J. Am. Chem. Soc.*, 1990, **112**(24), 8719-8733.
35 K. Jug, R. Iffert, *J. Mol. Struct. (Theochem)*, 1989, **186**, 347-359.
36 J. Kao, *Inorg. Chem.*, 1977, **16**(8), 2085-2089.
37 D.J. Meschi, R.J. Myers, *J. Mol. Spectrosc.*, 1959, **3**, 405-416.
38 S.E. Tarling, P. Barnes, J. Klinowski, *Acta Cryst.*, 1988, **B44**, 128-135.
39 N.Chr. Nielsen, H. Bildsoe, H.J. Jakobsen, P. Norby, *Zeolites*, 1991, **11**, 622-632.
40 P.J. Mead, M.T. Weller, *Zeolites*, 1995, **15**, 561-568.
41 S. Werner, S. Barth, R. Jordan, H, Schulz, *Z. Kristallogr.*, 1996, **211**, 158-162.

42 J. Flesche, S. Luger, P. Fischer, *Acta Cryst.*, 1987, **C43**, 809-811.
43 J. Lons, H. Schulz, *Acta Cryst.*, 1967, **23**, 434-436.
44 A. Gavezotti, *J. Am. Chem. Soc.*, 1983, **105** (16), 5220.
45 A. Bondi, *J. Phys. Chem.*, 1964, **68** (3), 441-451.
46 R.D. Shannon, *Acta Cryst.*, 1976, **A32**, 751-767.
47 *HyperChem*, ver. 6.03 for Windows, distributed by HyperCube Inc, 2000.
48 W. Von Niessen, P. Tomasello, *J. Chem. Phys.*, 1987, **87**(9), 5333-5337.
49 C. Heinemann, W. Koch, G-G. Lindner, D. Reinen, *Phys. Rev. A*, **52**(2), 1024-1038, (1995).
50 H. Rau, T.R.N. Kutty, J.R.F. Guedes de Carvalho, *J. Chem. Thermodynamics*, 1973, **5**, 833-844.
51 L. Pauling, *Proc. Nat. Acad. Sci. USA*, 1949, **35**(9), 495-499.
52 W. Von Niessen, *J. Chem. Phys.*, 1991, **95**(11), 8301-8308.
53 A.A. Landman, D. De Waal, *Crystal Engineering*, 2001, **4**, 159-169.
54 M.W. Wong, R. Steudal, *Chem. Phys Lett.*, 2003, **379**, 162-169.